International Journal of Modern Manufacturing Technologies
ISSN 2067–3604, Vol. XVI, No. 3 / 2024
https://doi.org/ 10.54684/ijmmt.2024.16.3.32

AN ENGINEERING MODEL FOR PRESSURE ASSESSMENT IN ROUGH CONTACTS

Delia Cerlinca[1,2], Sergiu Spinu[1,2]

[1] Department of Mechanics and Technologies, Stefan cel Mare University of Suceava,
13th University Street, 720229, Romania
[2] Integrated Center for Research, Development and Innovation in Advanced Materials, Nanotechnologies, and Distributed Systems for Fabrication and Control (MANSiD), Stefan cel Mare University, Suceava, Romania

Corresponding author: Sergiu Spinu, sergiu.spinu@fim.usv.ro

Abstract: In many scenarios involving mechanical contacts loaded in the elastic-plastic domain, finding the pressure distribution and the related stresses without a detailed description of the plastic strains may be a sufficiently good approximation for the contact problem solution. This approach is considered in this work, which aims to achieve a rapid solution for the pressure distribution in elastic-plastic contacts without the solution of the residual part: the influence of the plastic strains on the contact geometry, i.e., the residual displacements, and on the subsurface stresses, i.e., the residual stresses, are not accounted for. Experimental works and numerical approaches from the literature prove that the pressure in elastic-plastic contacts is limited to roughly three times the yield strength of the softer material. The latter threshold is introduced in a previously developed computer code for the purely elastic contact, as an additional restriction. The elastic-plastic pressure is calculated from the solution of the purely elastic problem, but it is not allowed to exceed the aforementioned limit. Considering the iterative nature of the original elastic solver, algorithm convergence is not affected by the additional restriction. The technique is firstly applied to a Hertz-type contact to prove the solution viability. A roughness sample is then processed with the newly advanced computer program. The resulting pressure distribution is compared to the purely elastic case. Considering that the former was achieved with the same computational effort as the latter, it is clearly a more convenient solution for practical engineering purposes.

Key words: rough contact, elastic-plastic, pressure distribution, yield strength, conjugate gradient method.

1. INTRODUCTION

Finding the pressure distribution established in the contact region when load is transmitted between two contacting bodies is a fundamental topic in mechanical engineering, as contact wear and damage reduce dramatically the service life of the contacting components. This is especially true when the limiting surfaces of the bodies do not conform, as in gears and bearings, due to high gradients of stress that develop in a small vicinity of the initial point (or line) of contact. Moreover, even modern manufacturing and finishing technologies can only reduce, but not completely eliminate, the inherent roughness. In this context, the contact between real surfaces is in the first stage established between the peaks of the microgeometry, which are unlikely to behave elastically regardless of the transmitted load.

On the other hand, a rigorous treatment of the peaks as individual elastic-plastic contacts generating plastic strains is not practical from an engineering point of view, because even modern imaging devices, such as optical profilometers, cannot extract enough information as to fully characterize each asperity. Moreover, the computational burden related to such fine discretization challenges the solution of the elastic-plastic contact, which can only be achieved numerically.

The pioneering work of Mayeur [1] allowed the tackling of the elastic-plastic contact problem with a deterministic approach, as opposed to the previous statistical endeavors. The modern semi-analytical approach in studying the rough elastic or elastic-plastic contact is based on the works of Polonsky and Keer [2], who advanced a robust algorithm for solving rough contact problems in the elastic domain, and on the three-dimensional semi-analytical elastic-plastic contact code developed by Jacq et al [3]. The method of Discrete Convolution and Fast Fourier Transform [4,5] made a significant contribution to the acceleration of the computation by offloading the convolution calculations to the frequency domain. Wang and Keer (6) investigated the effect of various strain-hardening laws on the elastic-plastic indentation behavior of materials, whereas Boucly et al [7] considered the

rolling and sliding motion of the contacting bodies by solving the elastic-plastic contact at each time step while upgrading the geometries as well as the hardening state along the moving directions. Chen et al [9] studied the interaction of nominally flat engineering surfaces with the assistance of the continuous convolution and Fourier transform algorithm. They derived empirical formulas for average gap, contact area ratio, and plastically deformed volume as functions of surface statistical characteristics, material properties and a hardening parameter. Chen et al [9] advanced a three-dimensional numerical elastic-plastic model for the contact of nominally flat surfaces based on the periodic expandability of surface topography. Their model studies the asperity interactions with the aid of newly derived formulas for the frequency response functions describing elastic-plastic stresses and residual displacement, thus giving a detailed depiction of subsurface stress and strain fields caused by the contact load.
This paper aims to advance a method for the rapid derivation of the elastic plastic pressure distribution and contact area for a deterministic rough contact surface inputted as a matrix of discrete heights measured with an optical profilometer. Following literature results, a material dependent limit is imposed on the contact pressure derived from the purely elastic model. The method preserves the speed of convergence of the purely elastic contact solver on which is based, and thus can process large data sets with up to 2048 by 2048 discrete measurements.

2. CONTINUOUS AND DISCRETE PROBLEM MODEL

The equations governing any contact process are well known from [10], and apply regardless of the assumed behavior of the contacting materials (elastic, elastic-plastic or viscoelastic). When two bodies bounded by dissimilar (or non-conforming) and smooth surfaces are brought into contact, an initial contact area of vanishing magnitude is established, i.e., a line or point contact area. If load is further transmitted through the contact, the contacting bodies deform elastically, and a contact area develops around the initial point or line. This contact area grows with increasing load, but will remain small in comparison to the dimensions of the contacting bodies. The transmitted load is equilibrated by a pressure distribution acting on the contact area of each body, leading to a distribution of subsurface stresses. When the latter stresses surpass a material dependent threshold, plastic flow is initiated in the contacting bodies. In most cases, the pressure is distributed such as the maximum stress intensity is not reached on the contact area, but at a certain depth comparable to the magnitude of the contact area (e.g., half-radius of the contact area in a spherical contact). The plastic flow process results in a distribution of plastic strains that develop around the initial point of flow inception. With further load increase, the plastic region reaches surface and the contact functioning is severely modified and finally compromised.
The contact problem is reported to a Cartesian coordinate system (x_1, x_2, x_3) with the origin in the initial point of contact. The x_1 and x_2-axes, also referred to as the tangential directions, are chosen to better separate the contacting bodies, and x_3 is the normal contact direction, along which the transmitted load acts. Some assumptions are needed to simplify the otherwise very complex problem model. Firstly, the bodies are approximated with elastic half-spaces, as the contact area is small compared to the bulk body dimensions. Secondly, although the contact surface may be a curved one, it is assumed plane and included in the tangential plane (also referred to as the common plane of contact). One important consequence is that pressure is aligned with the normal contact direction x_3 all over the contact surface. Thirdly, friction is neglected, and consequently the static force equilibrium is written only along the normal direction. The latter assumption works best when the contacting bodies have similar elastic properties, but otherwise the tangential processes can have a non-trivial effect [11] on the contact area and the pressure distribution. Also, no tilting or torsion moments are allowed, implying that the pressure centroid and the applied normal load are aligned.
Let W denote the transmitted load level, p the pressure distribution, h the distance (measured along the normal direction) between the bounding surfaces, and A_C the contact area, which is a subdomain of the common plane of contact. Initially, when $W = 0$ and the contact area is a line or point, h is simply the distance between points from the two contacting surfaces, resting on the same vertical, and will be denoted as h_0. With increasing load, the gap h is affected by two processes:
1.Under load, the bodies deform in the vicinity of the contact region, and the surface points undergo displacements u with respect to the initial position. These displacements are also assumed as aligned with the normal contact direction, and result in a concavity around the contact region.
2.Regardless of the latter displacement, the bodies as bulks approach each other with a quantity ω, referred to as the rigid-body approach. It is the variation of the distance between points from the two bodies, resting on the same vertical but distant from the contact region.
From geometrical considerations, one can write the following interference equation:

$$h(x_1,x_2)=h_0(x_1,x_2)+u(x_1,x_2)-\omega, \tag{1}$$

which holds true regardless of the type of contact (elastic, elastic plastic or viscoelastic), as long as the displacement u is properly expressed. In a purely elastic contact, u depends on the material properties and on pressure [2,10], whereas in a elastic-plastic contact, the contribution of the plastic region, also referred to as the residual displacements, must also be considered [1,3]. The static force equilibrium under the aforementioned assumptions reduces to:

$$W=\int_{-\infty}^{\infty}\int_{-\infty}^{\infty} p(x_1,x_2)dx_1dx_2. \tag{2}$$

The problem boundary conditions reflect other assumptions taken to achieve a solvable mathematical model: (1) adhesion on the contact area is neglected, which is warranted for the contact between metallic materials, but not for robber, and (2) the bodies are continuous and thus are not allowed to penetrate each other. These provide two additional inequalities that must be simultaneously satisfied:

$$p(x_1,x_2)\geq 0\,,\, h(x_1,x_2)\geq 0. \tag{3}$$

A final boundary condition controls the contact or non-contact status of every point in the common plane of contact. If on any vertical there exist a gap between the bounding surfaces, i.e., $h(x_1,x_2)>0$, the vertical is located outside the contact area. On the other hand, the existence of a non-vanishing pressure implies that the considered point is in contact. Thus, considering the exclusive nature of the two conditions, one can write that:

$$p(x_1,x_2)h(x_1,x_2)=0\,. \tag{4}$$

In continuous form the model (1) - (4) is not solvable for arbitrary contact geometry h_0. For particular h_0 (sphere on sphere, sphere on flat, sphere on cylinder, cylinder on cylinder) there exist the Hertz solution, which was also derived by analogy with another physical process. A fully analytical solution was achieved only for the first two types of contacts. For arbitrary geometry, numerical analysis and model discretisation is required.

To this end, a uniform rectangular two-dimensional grid D is established in the common plane of contact, encompassing the initial point of contact. The grid should cover a domain expected to include the contact area at the maximum load level. For each elementary domain, a representative point is chosen, and the vertical corresponding to the latter point is used to generate discrete counterparts for all problem parameters.

Further on, the elementary rectangles can be indexed using two integers, similar to a matrix notation, and the discrete distributions can be denoted using the said indexes. Essentially, continuous functions in the model (1) - (4) are replaced with two-dimensional arrays (matrices). In this framework, the contact area A_C is replicated by a reunion A of elementary rectangles, and the contact pressure, the gap and the displacement become piece-wise distributions uniform on each rectangle (but can vary from one elementary rectangle to the next). Using the indexes k,ℓ that vary from 1 to the number of grids N_1 and N_2 on each of the two directions, a discrete counterpart of the continuous model (1) - (4) can be written as:

$$\begin{cases} h_{k\ell}=u_{k\ell}+h0_{k\ell}-\omega, \quad (k,\ell)\in D; \\ W=\Delta\cdot\sum_{k=1}^{N_1}\sum_{\ell=1}^{N_2} p_{k\ell}, \quad (k,\ell)\in D; \\ h_{k\ell}=0,\ p_{k\ell}>0, \quad (k,\ell)\in A; \\ h_{k\ell}>0,\ p_{k\ell}=0, \quad (k,\ell)\in D\setminus A, \end{cases} \tag{5}$$

in which Δ is the area of the elementary rectangle, and A, D should be regarded as sets of indexes of elementary rectangles from the contact area, and from the considered grid, respectively. The model assumes that $A\subset D$, but $D\not\subset A$. Achieving the solution of the discrete model (5) means finding the set of indexes A of elementary rectangles in the contact area, and the pressure element for each of them. The application of this model to elastic-plastic contact is discussed in the following section.

3. SOLUTION STRATEGY AND ALGORITHM DESCRIPTION

The key to solving the contact problem is to properly express the displacements of points located on the boundaries of the contacting bodies, as well as the rigid-body approach ω. In the case of a purely elastic contact, the former is achieved [2] based on the half-space theory and on the Boussinesq solution for a normal point force acting on the half-space boundary. To this end, a matrix of influence coefficients is computed by integration of the latter solution over the elementary rectangle. Each influence coefficient expresses the displacement induced in a specific elementary rectangle, i.e. the observation cell, by a unity uniform pressure from another rectangle, i.e. the excitation rectangle. Thus, the influence coefficients depend on the distances between the observation and the excitation cells, and they must assume all possible values (each elementary cell must be treated as on observation, as well as an excitation point). A simplification occurs by observing that interchanging of the observation and excitation cells does not change the value of the influence coefficient. The elastic displacement can thus be expressed as [4]:

$$u_{ij} = \sum_{k=1}^{N_1} \sum_{\ell=1}^{N_2} K_{|i-k|,|j-\ell|} p_{k\ell} \, , \tag{6}$$

in which **K** is the influence coefficients matrix. It should be noted that, although **K** has the same size as **u** or **p**, K_{ij} is not related to the elementary cell of indexes (i, j), as u_{ij} and p_{ij} are. In fact, K_{ij} expresses a relation between any two elementary cells that are located at *i* elementary cells apart along $\vec{x}_1$ and at *j* elementary cells apart along $\vec{x}_2$. The use of the absolute value function in (6) is warranted by the fact that $K_{i-k,j-\ell} = K_{k-i,\ell-j}$, and avoids the use of negative indexes in matrix notation. By using the dummy function

$$k(x_1, x_2) = x_1 \ln\left(x_2 + \sqrt{x_1^2 + x_2^2}\right) + x_2 \ln\left(x_1 + \sqrt{x_1^2 + x_2^2}\right), \tag{7}$$

the matrix of influence coefficients **K** can be obtained:

$$K_{ij} = \frac{1-\nu}{E} \begin{pmatrix} k(x_1(i)+\Delta_1/2, x_2(j)+\Delta_2/2) + k(x_1(i)-\Delta_1/2, x_2(j)-\Delta_2/2)... \\ -k(x_1(i)+\Delta_1/2, x_2(j)-\Delta_2/2) - k(x_1(i)-\Delta_1/2, x_2(j)+\Delta_2/2) \end{pmatrix}. \tag{8}$$

Here, $x_1(i)$ and $x_2(j)$ are the coordinates of the centre of the elementary cell (i, j) along $\vec{x}_1$ and $\vec{x}_2$, respectively, ν and *E* are the elastic parameters of the material (Poisson's ratio and Young modulus, respectively), and Δ_1 and Δ_2 the side lengths of the elementary rectangle, thus $\Delta = \Delta_1 \Delta_2$.

Once the displacement is expressed as a function of pressure, an iterative approach can find the solution of the discrete model (5), and the most efficient algorithm remains to date the one proposed in [2]. Both contact area and pressure distribution are iterated simultaneously, resulting in increased speed of convergence, sustained by the modern numerical method applied for the linear system solution, namely the Conjugate Gradient method.

A computer code for the elastic plastic contact with isotropic hardening was recently developed by these authors [12]. In the latter, by using the Betti's reciprocal theorem, the displacement in an elastic plastic contact process was expressed as the sum two contributions: the elastic part calculated according to (6), and a residual part depending on the plastic strains developed during loading. As the volume with plastic strains in not known in advance, an iterative approach is needed, and the end result is an algorithm with three nested loops. The latter approach is appropriate for conceptual studying of the elastic-plastic contact problem with smooth contact geometry, but falls short when applied to rough contacts because of its computational complexity.

Modern measurement devices such as optical profilometers or atomic force microscopes can extract detailed information related to microtopography, resulting in large data that need to be processed for contact solution. Solving grids with 10^6 points in the common plane of contact can become overpowering even for modern computers, the main limiting factor being not the processing power of the CPU, but the size of RAM (it should be remembered that the grid needs to be extended in depth thus increasing the number of points with several orders of magnitude).

Moreover, in many cases, the step of the measurement device is not small enough as to capture the slope continuity of the scanned profile, and many peaks are created artificially due to lack of resolution. The high peaks will results in steep pressure gradients that are clearly unrealistic and a consequence of poor discretisation. Therefore, studying an elastic-plastic rough contact with a fully developed computer code like the one advanced in [12], although sound from a theoretical point of view, may be unpractical for engineering applications.

The literature on elastic-plastic contacts, supported by finite element analysis or by semi-analytical methods such as [1,3,6,7] applied to smooth contacts, suggests that the elastic-plastic pressure is similar to the one from the elastic case except for a limiting threshold depending on the contacting material. For practical calculations, three times the material yield limit σ_Y is considered a good enough approximation. It should be noted that the existence of a plateau of uniform pressure was also predicted by the computer code advanced by this author [12]. This is the consequence of the contribution of the residual displacement, which modifies the contact interference equation by increasing the contact conformity in specific regions, thus resulting in a more evenly distributed pressure over the contact area.

The result is exploited in this approach, by imposing a limit on the maximum pressure that can be achieved while solving the contact model (5) with the displacement (6). In other words, the residual displacement is not accounted for, and consequently a pressure and contact area solution can be achieved without studying the subsurface growth of the plastic volume. Of course, the obtained pressure will not be enough to assess the stress state in the contacting body, because the plastic strains and consequently the residual stresses will be unknown. However, it should be noted that as long as the elastic limit is not severely exceeded, the residual stresses are one order of magnitude smaller than the stresses due to contact pressure [13]. In many practical engineering scenarios, knowledge of the extension of contact area and of the pressure distribution provides enough information for assessing the contact strength. Without the need for a volume study, which would translate in a three-dimensional mesh, the contact model (5), coupled with the additional imposed inequality

$$p_{ij} \leq p_{\max} = 3\sigma_Y, \, (i,j) \in A. \tag{9}$$

form a model whose solution can be achieved with a similar computational effort as for the purely elastic case.

The base for solving the new contact model (5) and (9) is the algorithm [2], which is modified to account for the additional constraint (9). Considering that the original code allows for inequality constraints such as (3) and (4) to be imposed during the iterative process, the new condition (9) can also be added without a fundamentally altering the algorithm structure. The starting point is a contact solution in which all elementary cells are in contact and the associated pressure equals the average pressure over the entire grid. From this initial approximation, a displacement field is calculated that is introduced in the interference equation (1), resulting in a new pressure iteration. If the extensions of the contact area have been overestimated, the latter pressure contains both positive and negative values. However, (3) constrains pressure to be positive, thus the elementary cells with negative pressure are excluded from the contact area and their pressure is set to zero. At the next iteration, a new contact area and the associated pressure are found. A series of approximations are thus created, converging to the contact area and the pressure distribution that verify best the equilibrium equation (2).

From the aforementioned, one could conclude that the series of iterations approximate the contact area by overestimation only. A parallel process is implemented, in which, for every pressure, the calculated gap is compared to zero and the inequality (3) is also applied for gap: cells for which the gap results negative are reintroduced in the contact area. The reason for this is that, when the gap profile passes from positive to negative values, the boundary of the contact area is in between. Thus, a negative gap value suggests that the contact area is underestimated. One can notice that both constraints in (3) are imposed, leading to a series of approximations that should converge, from both upper and lower values, to the real contact area and pressure distribution. Once a solution that verifies all constraints and the static force equilibrium to an imposed precision, is found, it can be regarded as the problem solution, because of the uniqueness of solution in elastostatics problems.

Condition (9) is imposed by defining a new domain $Y \subset A \subset D$, on which, if the computed pressure is greater than the imposed threshold, it is set to the latter minus a quantity small enough as to not significantly disturb the static force equilibrium. In this manner, cells not only enter Y, but can also be excluded from it, assuring that the domain Y is thus iterated from both sides. The predictions of the newly designed computer code are verified and discussed in the following section.

4. METHOD VALIDATION AND APPLICATION TO ROUGH CONTACTS

Based on the aforementioned model and algorithm, a Matlab computer code was developed. The smooth spherical contact is first analysed, aiming to validate the found numerical predictions. The spherical contact of purely elastic materials is one of the few contact cases with analytical solution, and the numerically predicted pressure distribution matches well the Hertz solution for the contact radius a_H and the maximum central pressure p_H. The latter parameters are used as normalizers for radial coordinates and pressure distribution, respectively. Although the problem is reported to a Cartesian coordinate system, the depiction of pressure in figure 1 in radial coordinates is warranted by the fact that the spherical contact problem is axisymmetric. The contact simulation is then restarted with various thresholds σ_Y (see equation (9)) that are chosen as ratio to p_H, while keeping the normal load fixed. The predicted pressure distributions exhibit a central plateau of uniform pressure at the level of the imposed limiting pressure. The latter plateau mimics well the increase in contact conformity observed in [12] due to the residual displacement. The lower the threshold, the greater the contact area needed to support the contact load.

These authors [12] have previously advanced a computer code for the simulation of the elastic plastic contact with hardening behaviour, in which the pressure distribution and the contact area resulted by a three-dimensional study of the plastic strains and the residual stresses developed in the elastic-plastic material. In order to compare the predictions of the latter with the current simplified two-dimensional method, the hardening behaviour is neglected, and thus the function of the plastic strains $\sigma_Y(e^p)$ in equation (14) from [12] is replaced by a constant. The contact radii and the pressure profiles are then compared and a strong resemblance if found. The main differences are in the pressure profiles, at the boundary of the uniform pressure plateau Y, where the simplified method exhibits a slope discontinuity that is not present in the fully-fledged 3D model. The latter discontinuity is clearly a limitation of the 2D method. However, it should be noted that, for the same resolution N_1 by N_2, the solution of the newly advanced 2D is achieved in a few seconds, whereas that of the 3D model requires a few hours. But more important, on a computer with 32GB of RAM, the 2D model can run a 2048 by 2048 grid, whereas the 3D variant is limited to 256 by 256 by 256. Depending on the specific needs of the simulation, one or the other approach may be more suitable.

The strength of the newly advanced simplified model is the ability to rapidly process grids with high density of points as resulting from topography measurement devices. A roughness sample comprising an area of $0.1\,\text{mm}\times0.1\,\text{mm}$, containing 1024×1024 discrete height measurements, is simulated with the newly advanced code. Figure 2 depicts the initial gap h_0 inputted in the simulation. It should be noted that the points with the smallest coordinate along $\vec{x}_3$ are the first to enter contact. Figure 3 shows the pressure distribution and the contact area predicted with no limiting value, i.e. a purely elastic model, whereas in figure 4 a threshold $\sigma_Y = 1\,\text{GPa}$ was imposed. One can see that the contact spots in figure 3 are included in the contact area depicted in figure 4, and that the magnitude of the latter is orders of magnitude greater than the first.

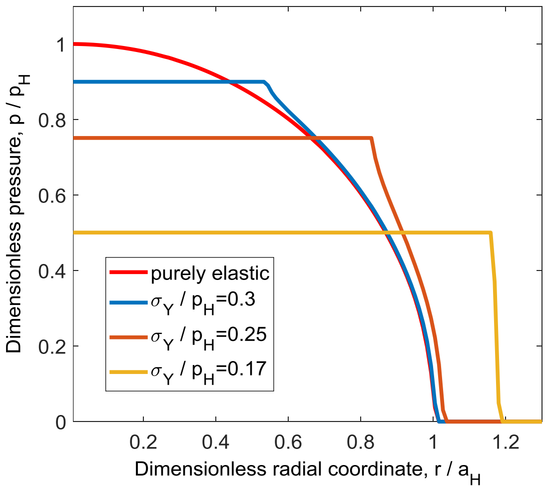

Fig. 1. Pressure radial profiles in a spherical contact

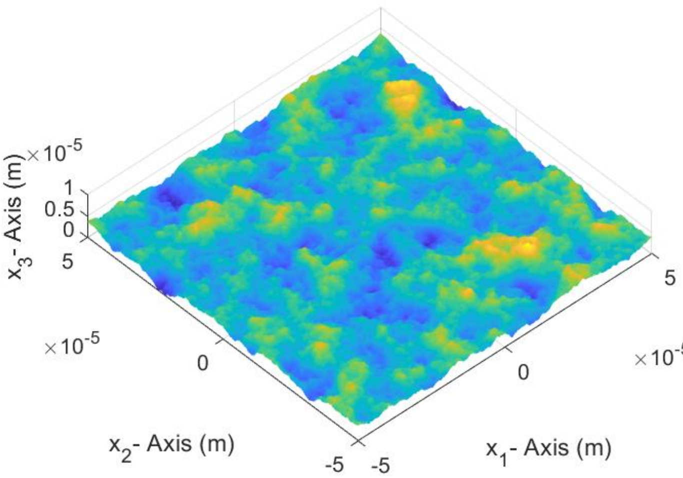

Fig. 2. Plot of the roughness sample h_0

For comparison purposes, the same axis limits for contact pressure were imposed in figures 3 and 4. The high pressure peaks in figure 3 are clearly unrealistic as the elastic material cannot withstand such stress without plastic deformation. It can also be asserted that the high pressure peaks are related to poor discretisation in the vicinity of the geometric peaks. The pressure distribution in figure 4 is a clearly more realistic solution for the rough contact problem. Although the permanent state of plastic strains and of residual stresses developing in the volume is not determined, surface parameters such as the pressure distribution and the contact area are efficiently assessed with a reasonable precision.

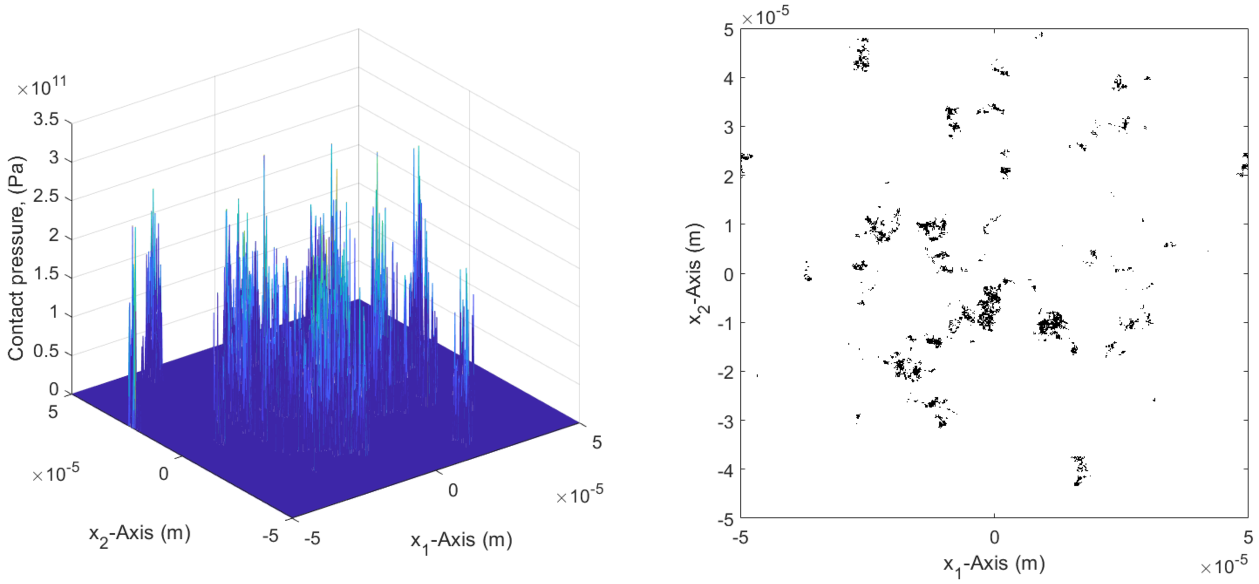

Fig. 3. Contact solution for the purely elastic model: pressure distribution (left) and contact area (right)

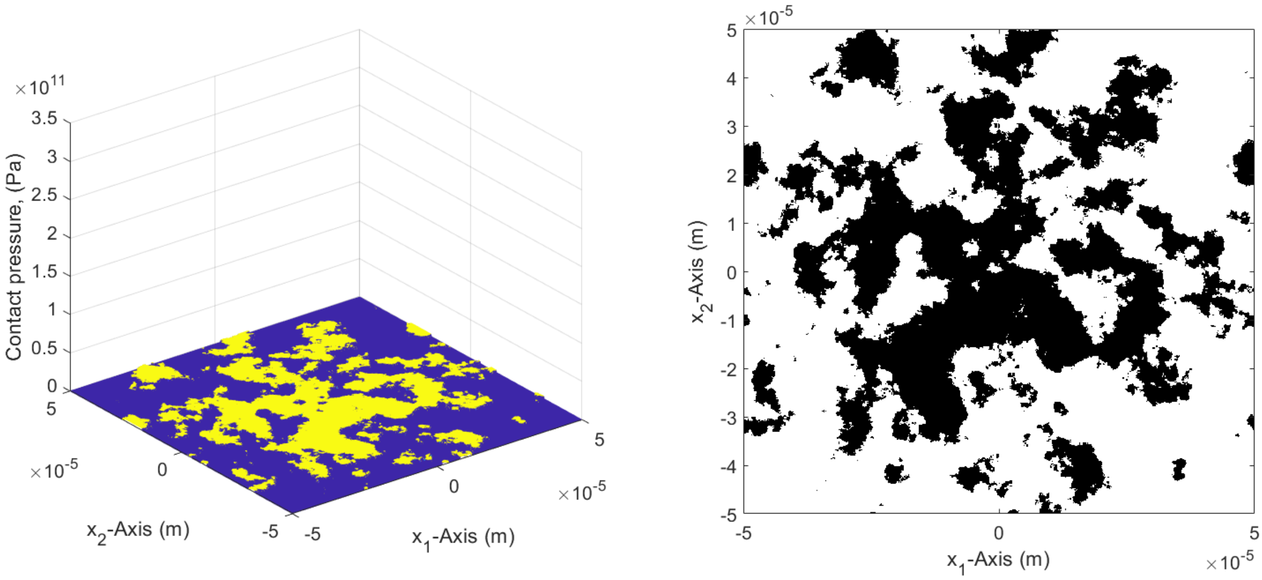

Fig. 4. Contact solution with a 3 GPa pressure limit: pressure distribution (left) and contact area (right)

5. CONCLUSIONS

Solving the smooth elastic-plastic contact problem with a volume analysis of the developing plastic strains and residual stresses helps advance the understanding of the involved processes, but the method cannot be directly applied to rough contacts due to lack of computational resources. Based on previous observations regarding the behaviour of the contact pressure in the presence of plastic strains, a simplified contact model is advanced in this paper.

The contact area and the pressure distribution are iterated simultaneously in a numerical scheme based on the Conjugate Gradient method. The displacement is calculated as in the purely elastic contact case. The problem discretisation allows for the treatment of arbitrary, yet known, contact geometry.

To account for the initiation of plastic yield in depth, a limit on pressure is imposed, related to the plastic yield limit of the material. This supplementary constraint results in a plateau of uniform pressure, simulating the contact behaviour in the presence of plastic strains and the contribution of the otherwise neglected residual displacement. The predicted pressure distribution is a reasonably accurate replica of the supposedly true pressure obtained by a

fully-fledged contact code, as proved by benchmarking with the smooth spherical contact.
The main advantage of the newly proposed approach is the computational efficiency. The simplified method is based on a two-dimensional discretisation of a region in the common plane of contact, whereas the full elastic-plastic study requires a three-dimensional discretisation of a volume comprising the plastic yield region. Two-dimensional grids with more than 2048 by 2048 points can be processed on modern personal computers, which is appropriate for rough contact simulations in practical engineering applications.

Funding: This paper has received no external funding.
Conflicts of Interest: There is no conflict of interest.

6. REFERENCES

1. Mayeur, C., (1995). Modelisation du contact rugueux elastoplastique (PhD Thesis, INSA Lyon, France).
2. Polonsky, I. A., Keer, L. M., (1999). *A Numerical Method for Solving Rough Contact Problems Based on the Multi-Level Multi-Summation and Conjugate Gradient Techniques*, Wear, 231(2) 206.
3. Jacq, C., Nelias, D., Lormand, G., Girodin, D., (2002). *Development of a Three-Dimensional Semi-Analytical Elastic-Plastic Contact Code*, ASME Journal of Tribology, 124 653-667.
4. Liu, S. B., Wang, Q., and Liu, G., (2000). *A Versatile Method of Discrete Convolution and FFT (DC-FFT) for Contact Analyses*, Wear, 243(1–2) 101–110.
5. Liu, S., Wang, Q., (2001). *Studying Contact Stress Fields Caused by Surface Tractions with a Discrete Convolution and Fast Fourier Transform Algorithm*, ASME J. Tribol., 124 36-45.
6. Wang, F., Keer, L. M., (2005). *Numerical Simulation for Three Dimensional Elastic-Plastic Contact with Hardening Behavior*, ASME Journal of Tribology, 127, 494-502.
7. Boucly, V., Nélias, D., and Green, I., (2007). *Modeling of the Rolling and Sliding Contact Between Two Asperities* ASME J. Tribol., 129, 235 – 245.
8. Chen, W. W., Wang, Q. J., Liu, Y., Chen, W., Cao, J., Xia, C., Talwar, R., and Lederich, R., (2007). *Analysis and Convenient Formulas for Elasto-Plastic Contacts of Nominally Flat Surfaces: Average Gap, Contact Area Ratio, and Plastically Deformed Volume*, Tribol. Lett., 28, 27–38.
9. Chen, W. W., Liu, S., Wang, Q. J., (2008). *Fast Fourier Transform Based Numerical Methods for Elasto-Plastic Contacts of Nominally Flat Surfaces*, ASME J. Tribol., 75, 011022.
10. Johnson, K. L., (1985). Contact Mechanics (Cambridge: University Press).
11. Spinu, S., Glovnea, M., (2012). *Numerical Analysis of Fretting Contact between Dissimilar Elastic Materials*, Journal of the Balkan Tribological Association, 18(2), 195-206.
12. Cerlinca, D., Spinu, S., (2022). *Numerical Simulation of Elastic-Plastic Contact with Isotropic Hardening*, International Journal of Modern Manufacturing Technologies, 14(2), 294 – 301.
13. Spinu, S., (2014). *A Robust Algorithm to Compute Residual Stresses in Elastic-Plastic Contacts*, Journal of The Balkan Tribological Association, 20(1), 63-74.

Received: March 18th, 2024 / Accepted: December 15th, 2024 / Paper available online: December 20th, 2024 © International Journal of Modern Manufacturing Technologies.